UNIVERSITY *of York*

This is a repository copy of *Biocatalytic Aromaticity-Breaking Epoxidation of Naphthalene*.

White Rose Research Online URL for this paper:
https://eprints.whiterose.ac.uk/id/eprint/171311/

Version: Published Version

Article:

White Rose
university consortium
Universities of Leeds, Sheffield & York

eprints@whiterose.ac.uk
https://eprints.whiterose.ac.uk/

Research Article

Biocatalytic Aromaticity-Breaking Epoxidation of Naphthalene and Nucleophilic Ring-Opening Reactions

Wuyuan Zhang,* Huanhuan Li, Sabry H. H. Younes, Patricia Gómez de Santos, Florian Tieves, Gideon Grogan, Martin Pabst, Miguel Alcalde, Adrian C. Whitwood, and Frank Hollmann*

Read Online

ACCESS | Metrics & More | Article Recommendations | Supporting Information

ABSTRACT: Aromatic hydroxylation reactions catalyzed by heme-thiolate enzymes proceed via an epoxide intermediate. These aromatic epoxides could be valuable building blocks for organic synthesis giving access to a range of chiral trans-disubstituted cyclohexadiene synthons. Here, we show that naphthalene epoxides generated by fungal peroxygenases can be subjected to nucleophilic ring opening, yielding non-racemic trans-disubstituted cyclohexadiene derivates, which in turn can be used for further chemical transformations. This approach may represent a promising shortcut for the synthesis of natural products and APIs.

KEYWORDS: arene epoxides, arene oxyfunctionalization, biocatalysis, chemoenzymatic reactions, naphthalene epoxides, oxidation, peroxygenase
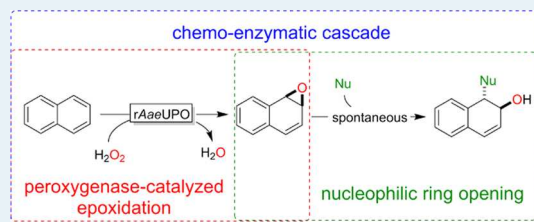
Aromatic systems are thermodynamically and kinetically very inert. Reactions breaking aromaticity are rare but interesting from a preparative point of view.[1,2] Even less common are enzymatic aromaticity-breaking reactions. Non-heme Fe-dioxygenases have been reported for stereoselective cis-dihydroxylation of arenes.[3−5] More recently, enzymatic Birch-type reductions[6−8] and dearomatizing arene oxidations[9] have also been reported.

Aromatic hydroxylation reactions catalyzed by heme-dependent enzymes such as P450 monooxygenases[10] and related peroxygenases[11−15] are well known to proceed via an intermediate, short-lived arene oxide prone to rapid, spontaneous rearrangement into the corresponding phenol products (known as NIH-shift, Scheme 1b).[10] Interestingly, capturing the intermediate arene oxides with nucleophiles has so far not been considered. This is unfortunate as arene oxides are potentially very useful building blocks for chemical synthesis. Nucleophilic opening of the reactive epoxide ring leads to trans-disubstituted cyclohexadiene derivates, which can serve as starting materials for various syntheses.[16−20] Their synthetic relevance today, however, is limited due to tedious, multistep synthesis protocols (Scheme 1a).[21−23] Utilizing heme-enzyme-derived aromatic epoxides, which are formed directly from the corresponding arenes under mild conditions, would give a more straightforward access to such trans-disubstituted cyclohexadiene derivates.
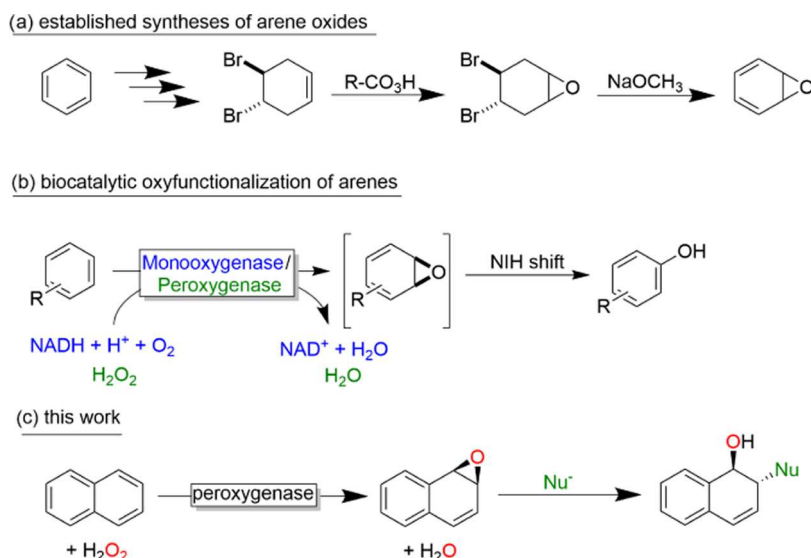
We therefore set out to investigate whether trans-disubstituted cyclohexadiene derivatives can be obtained in a chemoenzymatic reaction comprising enzymatic formation of arene oxides followed by nucleophilic epoxide opening (Scheme 1c). As a starting point, we chose the recombinant,

evolved peroxygenase from Agrocybe aegerita (rAaeUPO) as a catalyst; more specifically, we first used a previously evolved variant (PaDa-I).[24] Naphthalene was used as a starting material.[11] Upon addition of PaDa-I (0.2 μM_{final}) to a buffered solution of naphthalene and H_2O_2 (2 mM each), we could detect (and quantify) naphthalene-1,2-epoxide (**2**) via its characteristic absorption band at 266 nm.[25] **2** was relatively stable and rearranged into the corresponding 1-naphthol within several minutes (Figures S30 and S31). The epoxide formation rate correlated with the concentration of the biocatalyst (Table 1, entries 1−3). Increasing the H_2O_2 concentration above 2 mM resulted in a decreased concentration of **2** (Table 1, entries 2, 4, and 5), which is readily explained by the oxidative inactivation of heme enzymes by excess H_2O_2.[26] Further investigations will focus on determining the kinetic parameters of the enzyme-catalyzed epoxidation reaction. No epoxide formation was observed in the absence of PaDa-I, naphthalene, or H_2O_2. Isotope labeling experiments using $H_2^{18}O_2$ confirmed that the oxygen atom incorporated originated from H_2O_2 (Figure S27).

The decay of the intermediate epoxide accelerated upon addition of azide, which we interpreted to be the result of nucleophilic ring opening. Next, we investigated the factors influencing the overall yield in the desired addition product

Scheme 1. Synthesis of Arene Oxides[a]

(a) established syntheses of arene oxides

(b) biocatalytic oxyfunctionalization of arenes

(c) this work

[a](a) The established, multistep synthesis of arene oxides at the example of benzene oxide. (b) Heme-enzyme-catalyzed oxyfunctionalisation of aromatic compounds (e.g., benzene) proceeds via an intermediate arene epoxide spontaneously rearranging into the corresponding phenol; (c) In this work, we demonstrate that the intermediate arene oxides (e.g., obtained from peroxygenase-catalyzed transformation of naphthalene) can be reacted with nucleophiles, yielding chiral trans-disubstituted cyclohexadiene derivates.

(**4a**) (Table 1). Increasing the nucleophile concentration significantly shifted the ratio of the desired (**4a**) to the undesired (**3**) (Table 1, entries 6−9). Prolonging the reaction time allocated to the enzymatic epoxidation had no significant influence on the overall conversion of the naphthalene starting material (ranging between 80 and 85%, Table 1, entries 10−13) but increased the yield in the undesired rearrangement product 1-naphthol (**3**). Adding NaN$_3$ from the beginning of the reaction resulted in the complete recovery of the naphthalene starting material, which we attribute to the N$_3^-$-related inactivation of the heme enzyme. It is worth mentioning that the azide attacked the epoxide selectively at the C1 position (yielding the 1-azido-2-ol product). This selectivity was observed only with epoxide **2** and we are currently lacking a plausible explanation for this peculiarity.

From a semi-preparative reaction of 1-bromonaphthalene, approximately 39 mg of essentially pure (1S,2S)-2-azido-5-bromo-1,2-dihydronaphthalen-1-ol was isolated (73% isolated yield), crystallized, and analyzed via X-ray crystallography (see the Supporting Information for further details). The structure of the ring-opened product **4b** showed an excellent Flack parameter [−0.02(3)], thus allowing the determination of the absolute configuration ((1S,2S)-2-azido-5-bromo-1,2-dihydronaphthalen-1-ol). This corresponds well with the predicted stereoselectivity of the PaDa-I-catalyzed epoxidation of naphthalene (Figure 1B). Also, the crystallization of **4a** was successful; however, probably due to the lack of a heavy atom in the structure, the crystalized product **4a** showed a less convincing configuration (Flack) parameter [−0.3(3)]. As mentioned above, the ring opening occurred via a nucleophilic attack in the C2 position.

To further explore the substrate scope of the proposed reaction sequence, a range of naphthalene derivatives were evaluated (Figure 2). Using azide as a nucleophile, the yields ranged between 19 and 75%; products **4a**, **4b**, **4c**, **4d**, and **4e** were prepared on a semi-synthetic (0.2 mmol) scale (for full experimental details as well as ^{1}H NMR, ^{13}C NMR, ^{1}H−^{1}H

COSY, and HMQC-analysis of the products, see Figures S1−22). The isolated yields ranged between 20 and 73% giving access to 20−50 mg of the products, thereby correlating with the above-determined NMR-yields. So far, only the crystal structure of **4b** is available, and we compared the circular dichroism spectra of some representative products (i.e., **4d**, **4g**, and **4i**) with the CD spectrum of **4b** (Figures S32 and S33). The congruence of the optical rotatory dispersion curves suggests an identical (1S, 2S) configuration of these products as well.

In an attempt to also broaden the nucleophile scope of the reaction, we tested formate as an alternative nucleophile (Figure 2, **4j** and **4k**). The isolated yields, however, were significantly lower (9−15%) than observed using azide, which most likely can be attributed to the poorer nucleophilicity of formate as compared to azide under the reaction conditions.

Aiming at extending the arene scope of the proposed chemoenzymatic reaction sequence, we also evaluated benzene as the starting material. PaDa-I, the rAaeUPO variant used so far, exhibited poor activity with benzene (Figure 2, **4m**, blue). We therefore also evaluated the SoLo variant (engineered from PaDa-I)[27] for the transformation of benzene (Figure 2, **4m**, green). The significantly higher activity of SoLo on benzene (48% yield) compared to PaDa-I (traces) can be rationalized by its modified active site geometry: SoLo carries two mutations at the heme access channel (F191S and G241D, Figure 3). Possibly, the G241D substitution induces a displacement in the α-helix hosting the catalytic acid−base pair (R189-E196). This conformational change may favor the positioning of smaller arenes (see docking simulations, Figure S34) and therefore facilitate the conversion of benzene.

Finally, we explored the synthetic possibilities of **4a**. Rearomatization proved to be astonishingly difficult as only concentrated perchloric acid enabled the full conversion of the intermediate epoxide (**2**) into the aromatic azide (**5**) (Figure 4 and see also Table S1). In contrast, catalytic hydrogenation over Pd/C to form a compound (**7**, Figures S23 and S24) or

Table 1. Influence of Reaction Time and Nucleophile Concentration on the Proposed Epoxidation Ring-Opening Reaction

entry	c(PaDa-I) [nM]	c(H_2O_2) [mM]	c(2) [mM]	TON (PaDa-I)
		PaDa-I-catalyzed Epoxidation of Naphthalene		
1	100	2	0.82	8200
2	200	2	1.06	5300
3	400	2	1.29	3200
4	200	1	0.73	3650
5	200	4	0.91	4500

	c(NaN_3) [mM]	reaction time [min][b]	c(4a) [mM]	c(3) [mM]	TON (PaDa-I)
		Chemoenzymatic Reaction[c]			
6	31.3	2.5	0.61	0.36	3050
7	62.5	2.5	0.97	0.30	4850
8	125	2.5	1.48	0.16	7400
9	250	2.5	1.36	0.23	6800
10	125	3	1.42	0.19	7100
11	125	4	1.43	0.26	7250
12	125	6	1.34	0.30	6700
13	125	10	1.27	0.32	6350

[a]Reaction conditions: [naphthalene] = 2 mM, [H_2O_2] = 1−4 mM, and [PaDa-I] = 100−400 nM in NaPi buffer pH 7.0 (30% CH_3CN), 30 °C. The spectrum was recorded after diluting the solutions 100 times; an extinction coefficient of 8850 mM^{-1} cm^{-1} at 266.5 nm was used to calculate the concentration. [b]Time allocated for the enzymatic reaction step (i.e., prior NaN_3 addition). [c][Naphthalene] = 2 mM, [H_2O_2] = 2 mM, and [PaDa-I] = 200 nM in NaPi buffer pH 7.0 (30% CH_3CN), 30 °C. The reactions continued for another 4 h before further characterizations were performed; products were quantified by high-performance liquid chromatography (HPLC). TON = [mol$_{(4)}$ × mol$_{PaDa-I}$$^{-1}$].

Cu^I-catalyzed 1,3−dipolar cycloaddition with terminal alkynes (yielding products **8a** and **8b**, Figures S25 and S26) proved to be straightforward (Figure 4). **5** could be readily reduced into aromatic amine (**6**, Figure S28).

In this study, we have demonstrated that peroxygenases provide a convenient access to naphthalene epoxide and possibly further arene epoxides for the synthesis of chiral trans-disubstituted cyclohexadiene derivates.

■ EXPERIMENTAL SECTION

Biocatalyst Preparation. The expression of the r*Aae*UPO variants PaDa-I and SoLo was performed in recombinant *Pichia pastoris* following a previously described procedure.[28] The culture broth of *P. pastoris* cells containing the peroxygenase in the supernatant was centrifuged at 8000 rpm for 2 h at 4 °C. The supernatant was filtered through a 20 μm filter and kept at −80 °C until further use. A detailed description of the cultivation procedure can be found in the Supporting Information. The enzymes used in the study were essentially pure as confirmed by sodium dodecyl sulfate polyacrylamide gel electrophoresis (SDS-PAGE) in 12% gels stained with Coomassie Brilliant Blue R-250 (Figure S34).

Chemoenzymatic Reactions. A typical epoxidation reaction was performed at a 1 mL scale in NaPi buffer (100 mM, pH 7, containing 30% v/v acetonitrile as a cosolvent) at 25 °C. The reaction mixture contained an aromatic starting material (2 mM) and r*Aae*UPO (PaDa-I or SoLo 200 nM). Reactions were started by addition of H_2O_2 (2 mM final) and gently stirred for 2.5 min after which the nucleophile was added from a concentrated stock solution. After the completion of the reaction, the reaction mixture was extracted with an aliquot dichloromethane. The organic phase was dried over $MgSO_4$ and evaporated under reduced pressure. The crude product was purified over a silica column using 10% ethyl acetate in pentane/heptane as the eluent.

Crystal Structures of 4a and 4b. Diffraction data were collected at 110 K on an Oxford Diffraction SuperNova diffractometer with Cu Kα radiation (λ = 1.54184 Å) using an EOS CCD camera. The crystal was cooled with an Oxford Instruments Cryojet. Diffractometer control, data collection, initial unit cell determination, frame integration, and unit-cell refinement was carried out with "Crysalis".[29] Face-indexed absorption corrections were applied using spherical harmonics, implemented in the SCALE3 ABSPACK scaling algorithm.[30] OLEX2[31] was used for the overall structure solution, refinement, and preparation of computer graphics and
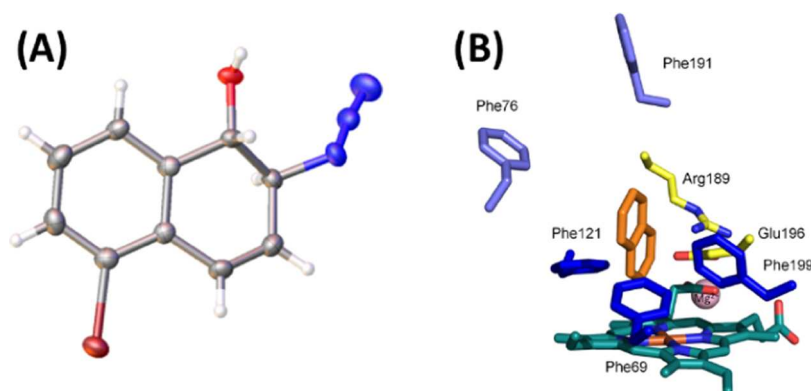

Figure 1. Crystal structure of (1S,2S)-2-azido-5-bromo-1,2-dihydronaphthalen-1-ol (A) obtained from the PaDa-I-catalyzed epoxidation of 1-Br-naphthalene followed by nucleophilic ring opening with NaN_3. (B) Active site model of PaDa-I in complex with naphthalene presenting the pro-(R)-face compound I. Naphthalene is placed between Phe121 and Phe199 in a T-packing mode with strong hydrophobic interaction with Phe69 that maintains a highly conserved orientation. Dark blue: Phe triad orienting the substrate, yellow: acid−base pair, and light blue: Phe pair involved in the guidance of the substrate to the active site.
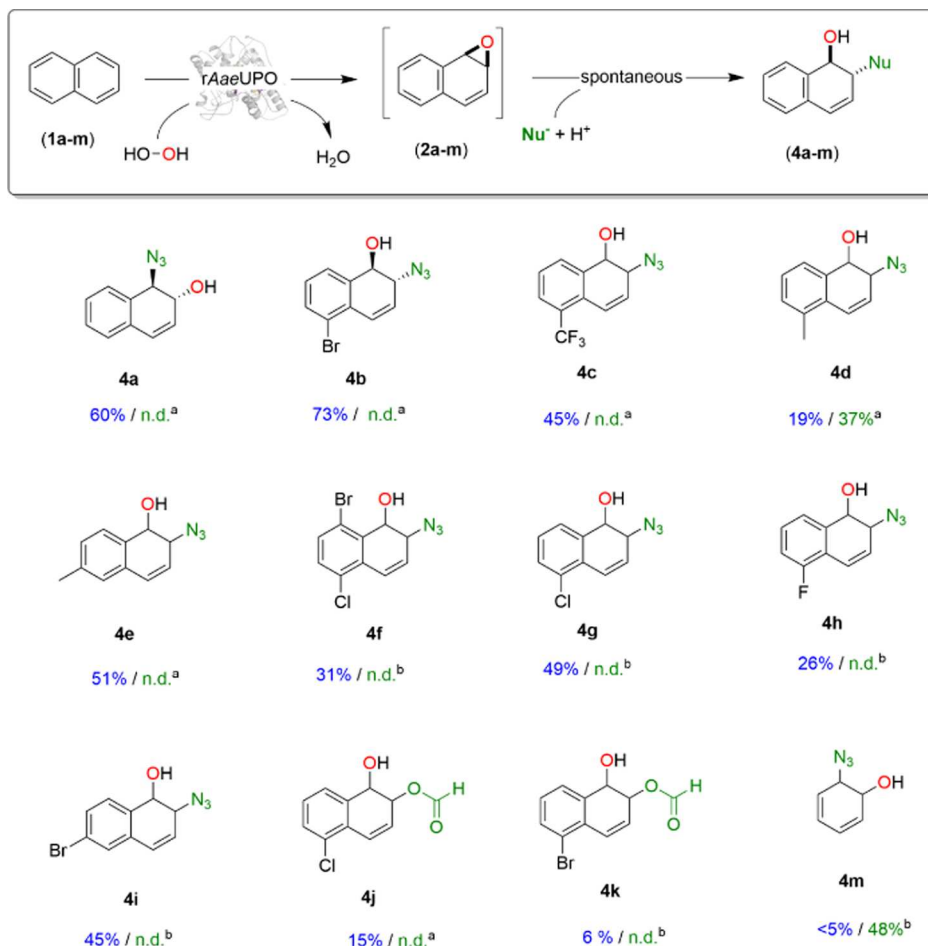
Figure 2. Preliminary product scope of the r*Aae*UPO variants PaDa-I and SoLo. Reaction conditions: [substrate] = 2 mM, [H_2O_2] = 2 mM, and [peroxygenase] = 200 nM in NaPi buffer pH 7.0 (30% CH_3CN), [NaN_3] = 125 mM, T = 30 °C. The conversion of benzene derivatives was determined by ^1H NMR. n.d.: not detected. a: isolated yield and structure confirmed by the crystal structure or 2D NMR; b: NMR-yield; characteristic peaks after ring opening (between 6.2 and 6.8 ppm) were used for the integration of the substrate, phenol as the side product, and diene as the product.
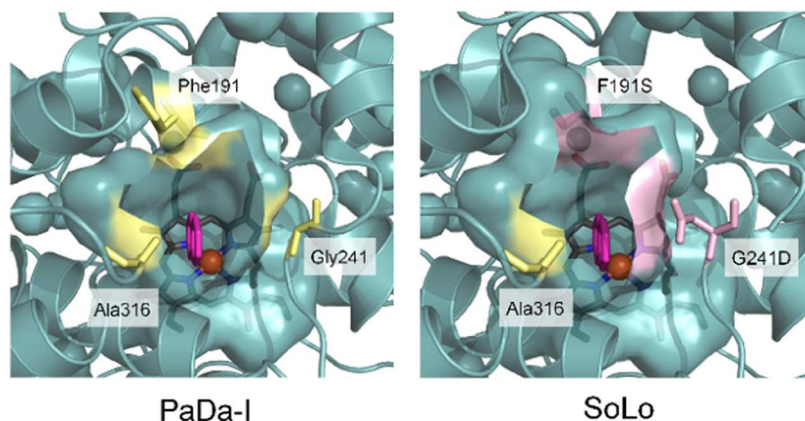

Figure 3. Active site models of the rAaeUPO variants used (PaDa-I, left and SoLo, right). The mutations in SoLo with respect to PaDa-I (F191S, G241D) are highlighted in pink.

publication data. Within OLEX2, the algorithm used for the structure solution was dual-space within ShelXT.[32] Refinement by full-matrix least-squares used the SHELXL[33] algorithm within OLEX2. All non-hydrogen atoms were refined anisotropically. Hydrogen atoms were placed by a difference map and refined.

Molecular docking simulations were performed using the Autodock VINA algorithm[34] included in YASARA Structure software.[35,36] Docking computations were performed at the level of the YASARA force field by running a number of 100 docking trials. Models were visualized with PyMOL Molecular Graphics System, Version 2.0 Schrödinger, LLC.
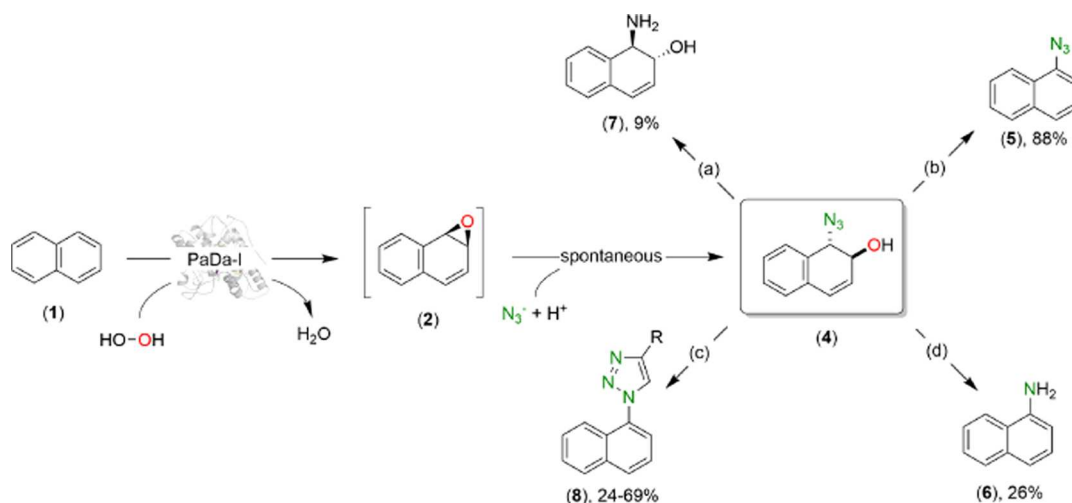
Figure 4. Exploring the synthetic potential of **4**. Reaction conditions: (a) Following the epoxidation and ring-opening reactions, the pH of the solution was then adjusted to approximately 9.0 using NaOH (5 M). The Pd/C catalyst (10 mol % final concentration) was added. N_2 gas was bubbled through the solution for 10 min, and a balloon of pure H_2 was applied to initiate the reduction. The reduction was carried out for 6 h. (b) Perchloric acid (3 M) was added after the epoxidation and ring-opening reactions and the mixture was stirred for 5 h. (c) Isolated azido alcohol **7** and alkyne (e.g., 1.5 equiv of phenylacetylene) were dissolved in H_2O and *tert*-butyl alcohol (2:1, v/v). $CuSO_4·5H_2O$ (5 mol %) and sodium ascorbate (10 mol %) were added. The reaction mixture was stirred for 8 h at 30 °C. (d) Sequence of reactions (b) and (a).

■ ASSOCIATED CONTENT

Ⓢ Supporting Information

The Supporting Information is available free of charge at

https://pubs.acs.org/doi/10.1021/acscatal.0c05588.

> Experimental procedures; analytical data; methods and synthetic procedures; X-ray crystallography; and determination of the absolute configuration (PDF)

■ AUTHOR INFORMATION

Corresponding Authors

Wuyuan Zhang − *Department of Biotechnology, Delft University of Technology, 2629HZ Delft, The Netherlands; Tianjin Institute of Industrial Biotechnology, Chinese Academy of Sciences, Tianjin 300308, China;* Ⓞ orcid.org/0000-0002-3182-5107; Email: zhangwy@tib.cas.cn

Frank Hollmann − *Department of Biotechnology, Delft University of Technology, 2629HZ Delft, The Netherlands;* Ⓞ orcid.org/0000-0003-4821-756X; Email: f.hollmann@tudelft.nl

Authors

Huanhuan Li − *School of Chemical Engineering and Technology, Xi'an Jiaotong University, Xi'an 710049, China*

Sabry H. H. Younes − *Department of Biotechnology, Delft University of Technology, 2629HZ Delft, The Netherlands; Department of Chemistry, Faculty of Sciences, Sohag University, Sohag 82524, Egypt*

Patricia Gómez de Santos − *Department of Biocatalysis, Institute of Catalysis, CSIC, 28049 Madrid, Spain*

Florian Tieves − *Department of Biotechnology, Delft University of Technology, 2629HZ Delft, The Netherlands*

Gideon Grogan − *York Structural Biology Laboratory, Department of Chemistry, University of York, YO10 5DD York, U.K.;* Ⓞ orcid.org/0000-0003-1383-7056

Martin Pabst − *Department of Biotechnology, Delft University of Technology, 2629HZ Delft, The Netherlands*

Miguel Alcalde − *Department of Biocatalysis, Institute of Catalysis, CSIC, 28049 Madrid, Spain;* Ⓞ orcid.org/0000-0001-6780-7616

Adrian C. Whitwood − *Department of Chemistry, University of York, YO10 5DD York, U.K.;* Ⓞ orcid.org/0000-0002-5132-5468

Complete contact information is available at:

https://pubs.acs.org/10.1021/acscatal.0c05588

Notes

The authors declare no competing financial interest.

■ REFERENCES

(1) Wertjes, W. C.; Southgate, E. H.; Sarlah, D. Recent advances in chemical dearomatization of nonactivated arenes. *Chem. Soc. Rev.* **2018**, *47*, 7996−8017.

(2) Hicks, J.; Vasko, P.; Goicoechea, J. M.; Aldridge, S. Synthesis, structure and reaction chemistry of a nucleophilic aluminyl anion. *Nature* **2018**, *557*, 92−95.

(3) Varghese, V.; Hudlicky, T. Short Chemoenzymatic Total Synthesis of ent-Hydromorphone: An Oxidative Dearomatization/ Intramolecular [4+2] Cycloaddition/Amination Sequence. *Angew. Chem., Int. Ed.* **2014**, *53*, 4355−4358.

(4) Hudlicky, T.; Reed, J. W. Celebrating 20 Years of SYNLETT-Special Account On the Merits of Biocatalysis and the Impact of Arene cis-Dihydrodiols on Enantioselective Synthesis. *Synlett* **2009**, *2009*, 685−703.

(5) Hudlicky, T.; Gonzalez, D.; Gibson, D. T. Enzymatic dihydroxylation of aromatics in enantioselective synthesis: Expanding asymmetric methodology. *Aldrichimica Acta* **1999**, *32*, 35−62.

(6) Kung, J. W.; Baumann, S.; von Bergen, M.; Muller, M.; Hagedoorn, P.-L.; Hagen, W. R.; Boll, M. Reversible Biological Birch Reduction at an Extremely Low Redox Potential. *J. Am. Chem. Soc.* **2010**, *132*, 9850−9856.

(7) Kung, J. W.; Loffler, C.; Dorner, K.; Heintz, D.; Gallien, S.; Van Dorsselaer, A.; Friedrich, T.; Boll, M. Identification and character-ization of the tungsten-containing class of benzoyl-coenzyme A reductases. *Proc. Natl. Acad. Sci. U.S.A.* **2009**, *106*, 17687−17692.

(8) Thiele, B.; Rieder, O.; Golding, B. T.; Muller, M.; Boll, M. Mechanism of Enzymatic Birch Reduction: Stereochemical Course and Exchange Reactions of Benzoyl-CoA Reductase. *J. Am. Chem. Soc.* **2008**, *130*, 14050−14051.

(9) Baker Dockrey, S. A.; Lukowski, A. L.; Becker, M. R.; Narayan, A. R. H. Biocatalytic site- and enantioselective oxidative dearomatiza-tion of phenols. *Nat. Chem.* **2018**, *10*, 119−125.

(10) Boyd, D. R.; Hamilton, J. T. G.; Sharma, N. D.; Harrison, J. S.; McRoberts, W. C.; Harper, D. B. Isolation of a stable benzene oxide from a fungal biotransformation and evidence for an 'NIH shift' of the carbomethoxy group during hydroxylation of methyl benzoates. *Chem. Commun.* **2000**, 1481−1482.

(11) Molina-Espeja, P.; Canellas, M.; Plou, F. J.; Hofrichter, M.; Lucas, F.; Guallar, V.; Alcalde, M. Synthesis of 1-Naphthol by a Natural Peroxygenase Engineered by Directed Evolution. *Chem-BioChem* **2016**, *17*, 341−349.

(12) Kluge, M.; Ullrich, R.; Scheibner, K.; Hofrichter, M. Formation of naphthalene hydrates in the enzymatic conversion of 1,2-dihydronaphthalene by two fungal peroxygenases and subsequent naphthalene formation. *J. Mol. Catal. B: Enzym.* **2014**, *103*, 56−60.

(13) Hofrichter, M.; Ullrich, R. Oxidations catalyzed by fungal peroxygenases. *Curr. Opin. Chem. Biol.* **2014**, *19*, 116−125.

(14) Barková, K.; Kinne, M.; Ullrich, R.; Hennig, L.; Fuchs, A.; Hofrichter, M. Regioselective hydroxylation of diverse flavonoids by an aromatic peroxygenase. *Tetrahedron* **2011**, *67*, 4874−4878.

(15) Pecyna, M. J.; Ullrich, R.; Bittner, B.; Clemens, A.; Scheibner, K.; Schubert, R.; Hofrichter, M. Molecular characterization of aromatic peroxygenase from *Agrocybe aegerita*. *Appl. Microbiol. Biotechnol.* **2009**, *84*, 885−897.

(16) McManus, M. J.; Berchtold, G. A.; Jerina, D. M. Nucleophilic addition of azide ion to benzene oxide: a reinvestigation. *J. Am. Chem. Soc.* **1985**, *107*, 2977−2978.

(17) Jeffrey, A. M.; Yeh, H. J. C.; Jerina, D. M.; DeMarinis, R. M.; Foster, C. H.; Piccolo, D. E.; Berchtold, G. A. Stereochemical course in reactions between nucleophiles and arene oxides. *J. Am. Chem. Soc.* **1974**, *96*, 6929−6937.

(18) Bertozzi, F.; Crotti, P.; Del Moro, F.; Feringa, B. L.; Macchia, F.; Pineschi, M. Unprecedented catalytic enantioselective trapping of arene oxides with dialkylzinc reagents. *Chem. Commun.* **2001**, 2606−2607.

(19) Rastetter, W. H.; Chancellor, T.; Richard, T. J. Biogenesis of epidithiadioxopiperazines. Nucleophilic additions to benzene oxide and sym-oxepin oxide. *J. Org. Chem.* **1982**, *47*, 1509−1512.

(20) Vogel, E.; Günther, H. Benzene Oxide-Oxepin Valence Tautomerism. *Angew. Chem., Int. Ed.* **1967**, *6*, 385−401.

(21) Yagi, H.; Jerina, D. M. General synthetic method for non-K-region arene oxides. *J. Am. Chem. Soc.* **1975**, *97*, 3185−3192.

(22) Gillard, J. R.; Newlands, M. J.; Bridson, J. N.; Burnell, D. J. Pi-facial Stereoselectivity in the Diels-Alder Reactions of Benzene Oxides. *Can. J. Chem.* **1991**, *69*, 1337−1343.

(23) Siddiqi, Z.; Wertjes, W. C.; Sarlah, D. Chemical Equivalent of Arene Monooxygenases: Dearomative Synthesis of Arene Oxides and Oxepines. *J. Am. Chem. Soc.* **2020**, *142*, 10125−10131.

(24) Molina-Espeja, P.; Garcia-Ruiz, E.; Gonzalez-Perez, D.; Ullrich, R.; Hofrichter, M.; Alcalde, M. Directed Evolution of Unspecific Peroxygenase from *Agrocybe aegerita*. *Appl. Environ. Microbiol.* **2014**, *80*, 3496−3507.

(25) Kluge, M.; Ullrich, R.; Dolge, C.; Scheibner, K.; Hofrichter, M. Hydroxylation of naphthalene by aromatic peroxygenase from *Agrocybe aegerita* proceeds via oxygen transfer from H_2O_2 and

intermediary epoxidation. *Appl. Microbiol. Biotechnol.* **2009**, *81*, 1071−1076.

(26) Burek, B. O. O.; Bormann, S.; Hollmann, F.; Bloh, J.; Holtmann, D. Hydrogen peroxide driven biocatalysis. *Green Chem.* **2019**, *21*, 3232−3249.

(27) Gomez de Santos, P.; Canellas, M.; Tieves, F.; Younes, S. H. H.; Molina-Espeja, P.; Hofrichter, M.; Hollmann, F.; Guallar, V.; Alcalde, M. Selective synthesis of the human drug metabolite 5′-hydroxypropranolol by an evolved self-sufficient peroxygenase. *ACS Catal.* **2018**, *8*, 4789−4799.

(28) Molina-Espeja, P.; Ma, S.; Mate, D. M.; Ludwig, R.; Alcalde, M. Tandem-yeast expression system for engineering and producing unspecific peroxygenase. *Enzyme Microb. Technol.* **2015**, *73*−*74*, 29−33.

(29) *CrysAlisPro*. Oxford Diffraction Ltd., Version 1.171.34.41.

(30) *Empirical Absorption Correction using Spherical Harmonics, Implemented in SCALE3 ABSPACK Scaling Algorithm within CrysAlisPro Software*. Oxford Diffraction Ltd., Version 1.171.34.40.

(31) Dolomanov, O. V.; Bourhis, L. J.; Gildea, R. J.; Howard, J. A. K.; Puschmann, H. OLEX2: a complete structure solution, refinement and analysis program. *J. Appl. Crystallogr.* **2009**, *42*, 339−341.

(32) Sheldrick, G. SHELXT - Integrated space-group and crystal-structure determination. *Acta Crystallogr., Sect. A: Found. Adv.* **2015**, *71*, 3−8.

(33) Sheldrick, G. A short history of SHELX. *Acta Crystallogr., Sect. A: Found. Adv.* **2008**, *64*, 112−122.

(34) Trott, O.; Olson, A. J. AutoDock Vina: Improving the speed and accuracy of docking with a new scoring function, efficient optimization, and multithreading. *J. Comput. Chem.* **2010**, *31*, 455−461.

(35) Krieger, E.; Vriend, G. YASARA View—molecular graphics for all devices—from smartphones to workstations. *Bioinformatics* **2014**, *30*, 2981−2982.

(36) Krieger, E.; Koraimann, G.; Vriend, G. Increasing the precision of comparative models with YASARA NOVA—a self-parameterizing force field. *Proteins* **2002**, *47*, 393−402.